Semin Immunopathol (2010) 32:275–287
DOI 10.1007/s00281-010-0216-x

REVIEW

Knocking at the brain's door: intravital two-photon imaging of autoreactive T cell interactions with CNS structures

Naoto Kawakami · Alexander Flügel

Received: 8 March 2010 / Accepted: 22 June 2010 / Published online: 11 July 2010

Abstract Since the first applications of two-photon microscopy in immunology 10 years ago, the number of studies using this advanced technology has increased dramatically. The two-photon microscope allows long-term visualization of cell motility in the living tissue with minimal phototoxicity. Using this technique, we examined brain autoantigen-specific T cell behavior in experimental autoimmune encephalitomyelitis, the animal model of human multiple sclerosis. Even before disease symptoms appear, the autoreactive T cells arrive at their target organ. There they crawl along the intraluminal surface of central nervous system (CNS) blood vessels before they extravasate. In the perivascular environment, the T cells meet phagocytes that present autoantigens. This contact activates the T cells to penetrate deep into the CNS parenchyma, where the infiltrated T cells again can find antigen, be further activated, and produce cytokines, resulting in massive immune cell recruitment and clinical disease.

Keywords Two-photon imaging · Autoimmunity · CNS

This article is published as part of the Special Issue on Immunoimaging of Immune System Function.

N. Kawakami (✉)
Department of Neuroimmunology,
Max-Planck-Institute of Neurobiology,
Am Klopferspitz 18,
82152 Martinsried, Germany
e-mail: kawakami@neuro.mpg.de

A. Flügel
Department of Neuroimmunology, Institute for Multiple Sclerosis Research, Faculty of University Medical Center Göttingen,
University of Göttingen and the Hertie Foundation,
Waldweg 33,
37073 Göttingen, Germany

EAE—an animal model of MS and tissue-specific autoimmunity

Multiple sclerosis (MS) is an autoimmune disease that is characterized by inflammation of the central nervous system (CNS). Although the detailed mechanism of MS is largely unknown, autoreactive T cells seem to play a central role in the pathogenesis of the disease. While a small number of autoreactive T cells also exist in healthy humans, they seemingly do not infiltrate into the CNS under normal conditions. The CNS has been considered an immune-privileged organ because it has no professional antigen-presenting cells (APCs) and no lymphatic vessels. However, this situation changes dramatically under inflammatory conditions, when lymphocytes including autoreactive T cells infiltrate into the CNS, and brain resident cells start to express molecules of the major histocompatibility complex (MHC) [1, 2]. Animal models of the disease have proven to be very powerful tools to study how autoreactive T cells start to attack the CNS [3]. Experimental autoimmune encephalomyelitis (EAE) is one of the most well-established and intensively studied animal models of human MS. EAE is either induced by active immunization with brain antigens emulsified in complete Freund's adjuvant [4] or by adoptive transfer of brain antigen-specific T cells [5]. Various antigens are commonly used to induce EAE, for example, myelin basic protein (MBP) [6], myelin oligodendrocyte glycoprotein (MOG) [7], or proteolipid protein (PLP) [8].

Lymphocytes have been shown to play an important role in EAE induction [9]. The adoptive transfer of lymph node (LN) cells derived from the CNS antigen-immunized animals into naïve recipients induces EAE. T cell depletion methods later showed that the T cell fraction

indeed facilitates this disease transfer [10]. In the 1980s, Ben-Nun et al. [5, 11] isolated the inducing element, autoantigen-specific T cells. MBP-specific T cells were cloned and expanded in vitro. After intravenous transfer of an MBP-specific T cell line, the animals developed paralytic symptoms, which occurred after a clinic-free period of 3–4 days.

Once the antigen-specific encephalitogenic T cells were established, many researchers tried to study the infiltration process into the CNS at a single-cell level. Hickey et al., for example, used histological methods [12], transferring in-vitro-activated T cells into syngeneic rats. Spinal cord cryosections were stained with antibodies against T cell antigens. Although they could detect early T cell infiltration, they could not distinguish if the T cells originated from the injected T cell population or from endogenous lymphocytes. To overcome this problem, they transferred MBP-specific Lewis T cells into Dark Agouti rats; exploiting allogenic markers, the transferred cells could be identified in the CNS of the recipient animals. Subsequently, radio isotope labeling (reviewed in [13]) was used: T cells were labeled with ^{111}In, and the radioactivity was measured in various organs 6 h after transfer and in this way T cell accumulation in the CNS was demonstrated in EAE rats. Although these methods could determine the amount of T cells in the organs, it was not possible to see each infiltrated cell.

In an earlier work, we established genetically labeled antigen-specific T cells for chasing a single cell [14]. In brief, green fluorescence protein (GFP) gene-coded cDNA was transduced into T cells using a retroviral vector. These GFP-labeled MBP-specific T cells ($T_{MBP\text{-}GFP}$ cells) keep their encephalitogenicity like nonlabeled MBP-specific T cells. Using $T_{MBP\text{-}GFP}$ cells, we demonstrated that they appeared in perithymic lymph nodes on day 1 posttransfer (p.t.) and in the spleen on day 2 p.t. before they arrived at the spinal cord on day 3 p.t. [15]. During their itinerary, $T_{MBP\text{-}GFP}$ cells underwent phenotypic changes, i.e., they downregulated activation markers and upregulated chemokine receptors. These steps appear to be important for migration into the CNS. As the analysis of the $T_{MBP\text{-}GFP}$ cells in the animal was only of “snap shot” quality, we subsequently used “real-time” analysis with two-photon microscopy.

Fluorescent labeling techniques for in vivo imaging

To analyze a defined population of cells, labeling must be done to distinguish other cell populations. For this purpose, fluorescent labeling techniques are most commonly used. Obviously, labeled cells have to be excited for efficient imaging. Therefore, excitation laser power and labeling techniques are equally important for high-quality imaging. Although two-photon excitation is not very phototoxic, higher-power lasers can cause damage. Since the two-photon laser is infrared, it can be used to warm up the sample (like a halogen heater). With better labeling, laser power and subsequent unnecessary tissue damage can be reduced and penetration depth increased. The common dyes for intravital imaging are listed in Table 1.

Long used in the analysis of cell division [16], carboxyfluorescein succinimidyl ester (CFSE) is one of most common chemical dyes for intravital imaging [17]. CFSE has a similar spectrum to that of fluorescein isothiocyanate (FITC). It is colorless and passively penetrates into living cells, where it is cleaved by esterases and becomes fluorescent. CFSE binds intracellular amines of the cellular proteins and acts as a long-term stable stain for cells. However, at too high concentration, it can disturb cellular function and may even kill the cells. Because CFSE binds stably to cellular proteins, labeled proteins are distributed evenly in the daughter cells which will then have half the fluorescence signal of the parental cell. Thus, CFSE is a very suitable fluorochrome for quantification of cell proliferation. At the same time, this property of the dye makes long-term imaging of actively dividing cells impracticable. 5-Chloromethylfluorescein diacetate (CMFDA) for green color and 5-(and-6)-(((4-chloromethyl)benzoyl)amino)tetramethylrhodamine (CMTMR) for red color represent alternative chemical dyes. CMFDA and CMTMR bind to thiols on proteins but still share the disadvantage of CFSE, i.e., they are diluted with cell divisions.

Stable labeling is necessary for long-term observation of dividing cells. For this purpose, cDNA coding for fluorescence protein (FP) is often inserted into the DNA of cells to establish stably transduced cells or transgenic animals. In general, this causes a weaker labeling than with chemical dyes, but since proteins are continuously synthesized, labeling is stable for a long time, even in dividing cells. One of the most famous and most common FPs is GFP. Originally cloned from jelly fish, it was optimized for brightness and eukaryotic expression by nucleotide modification [18, 19]. GFP matures in the cells without any cofactors and is quite stable. Most importantly, GFP can be expressed in living cells without disturbing cellular functions. In addition, ubiquitously GFP-expressing transgenic mice [20] and rats [21] have been established. GFP was modified further at the nucleotide level to obtain blue, cyan, and yellow fluorescence protein (BFP, CFP, and YFP, respectively) [22]. The classical red FP (RFP) was cloned from a coral [23]. It can be expressed equally as well as GFP, but it tends to multimerize, thus prohibiting its use as fusion protein. Furthermore, at high concentrations, it might exert cell toxicity. Recently, monomeric RFP and less toxic variants have been developed and employed for cell tracing

Table 1 Spectra of commonly used fluorescent markers for in vivo imaging

		2-photon excitation	Conventional excitation	Emission
Fluorescence proteins, jellyfish-derived	eBFP	780	380	440
	eCFP	860–920	433	475
	eGFP	880–930	488	509
	eYFP	960	513	527
Fluorescence proteins, coral-derived	Kaede (before conversion)	730	508	518
	Kaede (after conversion)	730	572	582
	tdTomato	900–1,000	554	581
	DsRed	930–990	558	583
	mCherry	760 or 900–1,000	587	610
Chemical dyes	CMF2HC	780–800	371	464
	CFSE	780–820	492	517
	CMFDA	800	492	517
	FITC	780–800	494	520
	CMTMR	780–820	541	565
	SNARF	700–810	563	639
	CMTPX	780–800	577	602
	Texas Red	780–920	595	615
Calcium indicator	Indo-1	700	346	475
	Indo-1 with Ca2+	700	330	401
	Fura-2	700–850	363	512
	Fura-2 with Ca2+	700–850	335	505
	Fura-4F	700–850	366	511
	Fura-4F with Ca2+	700–850	336	505
	TN-XXL	800	433	475
	TN-XXL with Ca2+	800	433	527
Visualization of organelles	Hoechst	780	350	461
	DAPI	700	358	461
	FM 1–43	830	480	565
	Rhodamine 123	780–860	507	529
	Dil	700	549	565
	Sulforhodamine 101	840–890	586	605
	DiD	780	644	665

in vivo. An interesting variant of RFP is Kaede. It can change from green to red after irradiation with UV light [24]. Since this photo conversion is stable for a long time, it can be very useful for tracking a particular single cell in vivo. Meanwhile, the repertoire of FPs has considerably widened, thereby making it possible to choose custom-tailored fluorochrome combinations for individual projects (reviewed in [25]).

During the intravital imaging, visualizing the environmental structure is very informative. For example, collagen fibers are visualized by second harmonic generation (SHG) [26]. SHG is a nonlinear coherent scattering process that conserves energy. SHG emission wavelength is always half the excitation wavelength. The blood vessel structures are commonly visualized by intravenous application of fluorescence-conjugated dextrans [27]. The molecular size of the dextran used must be large enough (>70 kDa) to prevent leakage from the blood vessels. Dextran fills the lumina of blood vessels but fails to mark endothelial cells. However, some phagocytic cells in the vessel surroundings can take up any dextran leaking out of the vessels and become fluorescent [28]. An attractive alternative label for the blood stream came with the commercial introduction of quantum dots (Q-dots), composed of a semiconductor nanocrystal with a special coating that improves its half-life in the circulation. Q-dots are efficiently excited at a broad range of wavelengths, have extraordinary photostability, and yield a strong fluorescence signal with a narrow emission spectrum [29]. Once excited by any wavelength, it emits a strong fluorescent signal. Since it is

extremely photo stable, Q-dot is suitable for long-term imaging. Moreover, there are dyes which label specific cells; for example, sulforhodamine101 labels only astrocytes [30].

Recently, a series of "functional" dyes have become available for visualizing intracellular calcium concentrations. New dyes are being developed for not only cell tracking but also visualizing cellular function such as intracellular signaling in vivo.

Two-photon laser scanning microscopy

During conventional ("single photon") excitation using confocal microscopy, a fluorescent molecule absorbs a photon with a specified energy. For example, a molecule of GFP absorbs a photon of 488-nm wavelength and becomes excited. After nonradiative relaxation, the molecule of GFP then emits a 509-nm photon and returns to basal energy state. In contrast, during two-photon excitation, a GFP is theoretically excited by two photons of 976-nm wavelength (488 nm×2), i.e., half the amount of energy of one photon with 488 nm (Fig. 1a). These two photons of 976-nm wavelength should arrive in a small volume (less than 1 f liter) over a short time period (scale of attoseconds) to achieve a two-photon effect. In such a situation, the energy of two independent photons can "fuse" to excite a GFP fluorochrome. Afterwards, GFP emits fluorescence as in the one-photon excitation. Fluorescent molecules show a wider excitation spectrum by two-photon excitation; for example, optimal excitation wavelength for GFP is shorter than 900 nm instead of 976 nm. Therefore, two fluorescence molecules with distinct excitation wavelengths, e.g., GFP and RFP, can both be excited by one wavelength of two-photon laser. In nature, a two-photon effect rarely occurs due to the enormous density of photons required for its generation. For example, under sunlight conditions, a rhodamine B fluorochrome will experience a one-photon excitation every second. In contrast, a two-photon effect will occur only once in ten million years [31].

Therefore, specialized lasers had to be developed for practical realization of two-photon laser scanning microscopy (TPLSM). Contrary to conventional lasers which produce photons spontaneously, these pulsed lasers can accumulate photons, emitting them from time to time. During this process, photons are concentrated within a 10-ns time window into 100 fs, which yields a 10^5-fold higher peak power, without changing the average power. These condensed photons are further focused by the objective lens of the microscope, leading to their maximal accumulation at the focal point. The theory of the two-photon effect was established in the early 1930s by Göppert-Mayer (reviewed in [32]). As high-power energy was required, the effect was experimentally confirmed only in 1961. Winfried Denk was the first to apply two-photon microscopy to biology in 1990 [33]. The resulting great breakthrough in biology research was due to the suitability of TPLSM for in vivo imaging.

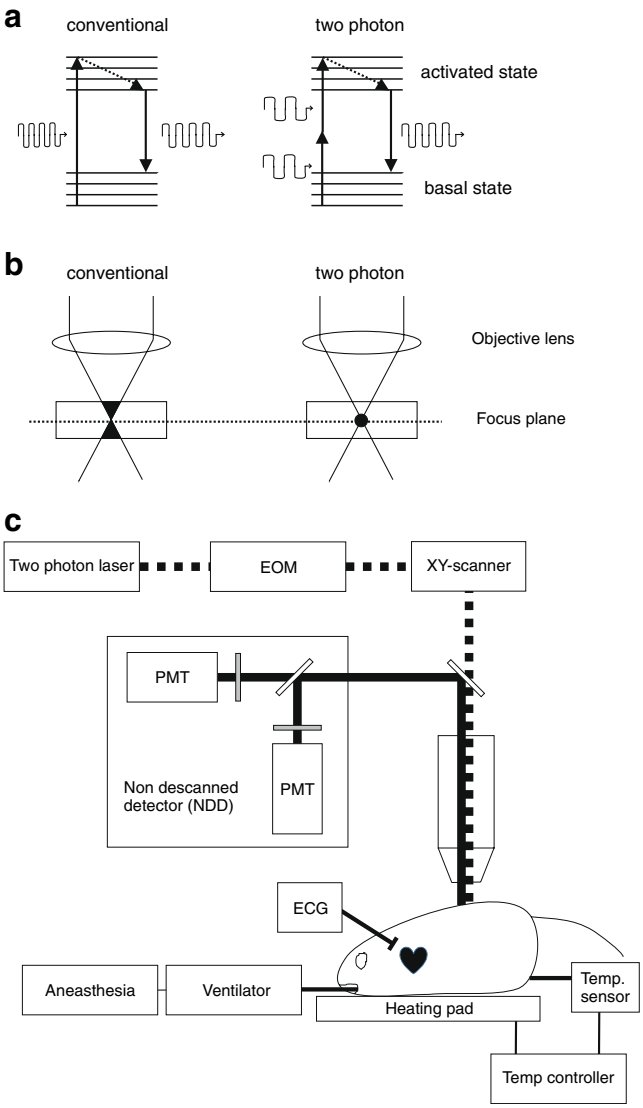

Fig. 1 **a**, **b** Comparison between conventional one-photon excitation versus two-photon excitation. **a** During conventional excitation, a photon activates a fluorescence molecule (*left*), whereas during two-photon excitation, two photons can sum up their energy to activate a fluorescence molecule (*right*). After nonradiative relaxation (*dotted line*), a fluorescence molecule emits fluorescence, which is common in both conventional and two-photon excitation. **b** Conventional laser can excite a fluorescence molecule on its way (indicated as *black area* in *left*). However, fluorescent molecules can be activated only at the focus point since two-photon effect needs energy accumulation (indicated as *black circle* in *right*). **c** CNS intravital imaging setup. The animal is anesthetized and respiration is controlled during the entire imaging session. Additionally, body temperature is kept at 37°C and ECG is monitored. Two-photon laser is routed to xy-scanner via EOM to control laser power. Thereafter, laser is focused by objective lens and reaches the sample. Emission is collected by the objective lens and detected by NDDs which are located immediately behind it

Since the two-photon effect occurs only at a focal point, there is little excitation outside the focal volume (Fig. 1b). Consequently, the fading of fluorescence is minimized. In addition, the pinhole for cutting fluorescence out of the focal plane in confocal microscopy is no longer necessary. Instead, TPLSM should detect all fluorescence signals regardless of whether they are scattered or not. Since scattering happens very frequently when imaging deep inside the tissue, the collection of scattered photons from the sample increases the detection sensitivity of the fluorescence signal. Furthermore, longer wavelength laser light (such as with two-photon excitation) is scattered less and therefore can penetrate more deeply into tissues. All in all, TPLSM is characterized by lower phototoxicity and higher penetration depth than one-photon microscopy such as confocal and fluorescence microscopy.

Confocal and two-photon systems equipped with photomultipliers as detectors can detect signals from one particular point simultaneously. A three-dimensional (3D) picture is obtained by scanning the laser through the sample in the x and y dimensions and then acquiring serial optical sections in a z-stack using a z-stepper motor to change the plane of focus in the sample. The time required to generate a 3D picture crucially depends on the speed of the scanner. Although newly developed resonance scanners reach velocities of up to 16,000 Hz (16,000 lines in 1 s), they are too slow to detect rapid biological events like intracellular calcium signaling. Thanks to newly developed techniques, two-photon lasers can now be split into multiple beams using sets of mirrors in the scanning unit while still retaining enough peak power. Scanning can be speeded up when the latter setup is combined with highly sensitive CCD detectors that can distinguish signals from multiple excited points [34].

Interesting technical innovations continue to be developed. For example, Helmchen et al. have miniaturized two-photon microscopy for mounting on living rats [35]. Using this system, they imaged the blood vessel structure in the brain and the calcium influx in neuronal cells. Although two-photon microscopy allows deep penetration, the depth is limited to approximately 1 mm. To overcome this limitation and allow deeper imaging, the gradient index (GRIN) lens was developed [36]. The GRIN lens has a needle-like shape and is attached to the surface of the objective lens. It permits imaging at a depth of 2 mm in the living animal with only minimal invasion.

Intravital imaging of immune reactions

A TPLSM hallmark study in immunology research was published in 2002 by Miller et al. [37]. By imaging naïve T and B cells in explanted lymph nodes, they compared T and B cell motility and demonstrated that the lymphocytes showed a "random walk" behavior in the absence of specific antigen. However, the T cells dramatically changed their motility pattern in the presence of antigen. T cells formed clusters, i.e., showed antigen recognition [37]. Concurrently, Bousso et al. demonstrated CD4/CD8 double-positive T cells by imaging them in thymic reaggregation culture [38]. Here, they showed MHC-dependent interactions between T cells and thymic stromal cells. Moreover, they also described long- and short-term dynamic interactions.

Although these well-documented studies had a very great impact in the field, they were not true in vivo studies. In 2003, Miller et al. performed the first intravital imaging of T cells [17], demonstrating naïve CD4 T cell motility in inguinal lymph nodes. T cells moved up to 25 μm/min and averaged a speed of 11 μm/min; interestingly, their locomotion behavior and their velocity resembled the one which had been observed before in explanted lymph nodes [37]. In later study, Bajénoff et al. showed that stromal cells guide T cells and keep them in the T cell zone of lymph node [39]. This suggests that T cell motility can be influenced by the surrounding structure. Subsequently, Mempel et al. [27] visualized the contact between naïve T cells ($CD4^+$ or $CD8^+$) and dendritic cells (DC) within popliteal lymph nodes. They proposed a three-step model of antigen encounter between T cells and DCs. According to this model, T cells make a series of short contacts with DCs at an early stage of antigen recognition (<8 h after antigen recognition). Thereafter (<24 h), T cells make a long stable contact and start to secrete cytokines. Finally, T cells detach from DCs and then start to move and make a short series of contacts (<48 h). During this stage, T cells proliferate. Similar multistep T–DC interactions were observed by Miller et al. using antigen-specific naïve $CD4^+$ T cells [40]. Furthermore, Shakhar et al. showed that this model was observed under priming and tolerance conditions [29].

Worbs et al. detected molecular signs of T cell motility in LN. They showed that the CCR7 ligands, CCL19 and CCL21, stimulate T cell motility [41]. T cells derived from CCR7-deficient mice exhibited reduced motility. In addition, T cells in plt/plt mice, which lack CCR7 ligands, also exhibited a slower motility but were rescued by CCL21.

Hugues et al. focused on $CD8^+$ T cells [42]. They demonstrated that the types of contact determine the functional outcomes. Short contacts induce tolerance, whereas long contacts activate T cells. Although they used lymph node explants, Bousso et al. showed the dynamic scanning process of dendritic cells and their interactions with $CD8^+$ T cells [43]. Slower than T cells, dendritic cells moved within the lymph nodes and made contacts with up to 500 T cells per hour and maximally ten T cells at same time. Miller et al., who used $CD4^+$ T cells instead of $CD8^+$

T cells [44], showed that dendritic cells scanned up to 5,000 CD4 T cells per hour and maximally 250 T cells simultaneously.

After interacting with dendritic cells, activated $CD8^+$ T cells show cytotoxic activity. Boissonnas et al. described how the arresting of $CD8^+$ T cells on tumor cells was antigen dependent [45]. Additionally, they demonstrated how the $CD8^+$ T cells resumed migrating after killing their target. Breart et al. showed in vivo killing of mouse tumors by adoptively transferred antigen-specific $CD8^+$ T cells [46]. They found that a CD8 T cell needed 6 h to kill one target tumor cell. Recently, Kim et al. demonstrated the motility of lymphocytic choriomeningitis virus infection-specific $CD8^+$ T cells at brain meninges during the viral infection [47]. They showed how $CD8^+$ T cells arrest the MHC-class-I-dependent pathway. They also illustrated leakage of the blood brain barrier (BBB) and showed how subsequently myelomonocytic cells infiltrated the CNS.

Intravital microscopy has been used to image not only T cell–DC interactions but also other combinations of interactions. Todokoro et al., for example, showed how regulatory T cells shorten interactions between primary $CD4^+$ T cells and DCs [48]. Qi et al. focused on B cells, showing how they surveyed antigen-bearing DCs [49]. B cells arrested on DCs and then induced intracellular calcium signaling. This interaction seemed to be important for antibody production, but not for germinal center formation. The same group demonstrated that the B–T cell interaction was necessary for the formation of a germinal center [50].

After T cells are stimulated in contact with antigen-presenting cells, T cells get activated. One of earliest hallmarks of activation is calcium influx. Bhakta et al. visualized calcium oscillations in the T cell [51]. They used thymic acute slices incubated with T cells that were labeled with calcium indicator. They nicely illustrated highly motile cells at low intracellular calcium concentration whereas arrested T cells after calcium spikes. Wei et al. showed similar founding that antigen/MHC-complex-induced calcium spikes arrested T cell motility in the explanted lymph node [52].

Two-photon imaging has also been used for subcellular resolution imaging. For example, Wei et al. [52] visualized intracellular calcium influx using $CD4^+$ T cells within lymph node explants. They demonstrated that $CD4^+$ T cells showed infrequent calcium spikes without specific antigen encounters. In contrast, T cells engaged with APCs presenting specific antigen showed an increased frequency of calcium spikes. These spikes persisted for hours independently of any contact with APCs. Other subcellular imaging studies were carried out by Dustin's group [53–56], who visualized a highly organized molecular distribution at the point of contact between T cells and APCs. This structure was called an immunological synapse, since it resembles neuronal synapses. These studies gave first valuable insights about the coordinated molecular rearrangements at the interface between T cell and APC in the course of T cell receptor signaling.

Intravital TPLSM of autoaggressive effector T cells

In the following, we want focus on recent findings about the in vivo behavior of brain antigen-reactive T cells. These studies gave new insights about the questions on how encephalitogenic T cells get access to the CNS and how these T cells interact with resident cells to initiate deleterious inflammation of the CNS tissue.

Our microscopy setup consists of a commercially available, tunable, pulsed two-photon laser system (Fig. 1c). A diode-pumped laser generates 10 W of continuous laser from Nd:YVO_4 crystals with a wavelength of 532 nm. This green laser is routed to Ti:sapphire laser, which converts the wavelength from 532 nm into femtosecond light pulses of 700–1,050-nm wavelength. The excitation wavelengths were tuned to the optimal excitation spectra of the used fluorochromes (Table 1), e.g., for the GFP/RFP combination, the laser was set to 935 nm. The laser power was controlled by an electrical optic modulator (EOM). A galvano mirror was employed for the xy scan of the tissue sample. The upright microscope was equipped with a 20-fold water immersion objective lens with a high numeric aperture (N.A. 0.95). Non-descanned detectors placed close to the objective ensured efficient sampling of the emitted fluorescent light (Fig. 1c). Up to four colors could be detected at the same time.

Animals were orotracheally intubated and anesthetized by isofluorane ventilation (concentration 1–2%). Fluorescence-labeled dextrans for visualization of blood vessels were injected i.v. via catheterization of the tail vein. For preparation of a spinal cord window, a 2–3-cm incision of the skin on the lumbar spine was performed, and the paravertebral musculature was removed. Thereafter, each animal was fixed stereotactically on a custom-made table. A laminectomy was carefully performed on one disk of the lumbar spinal cord (L1), leaving the dura intact. During the intravital recordings, physiological parameters, i.e., body temperature, blood gasses, pulse, and electrocardiogram (ECG), were constantly monitored. Images were acquired from an area typically 600 μm×600 μm at a depth of 30–50 μm (3–5-μm z-step). Repeated scanning and averaging were performed to minimize noise. Each scan took approximately 1.3 s per plane, yielding a total time interval of approximately 31 s. Using knock-out mice Kim et al. found that the chemokine receptor CXCR6 was not crucial for the formation of T cellular infiltrates during EAE [57]. Imaging in this study was performed through the intervertebral spaces

of the thoracic spine to avoid potential artifacts caused by the complete laminectomy. Comparing these preparation techniques we did not find significant changes in T cell locomotion pattern in early EAE lesions [28].

Intravascular T cell behavior in the CNS had been studied using intravital fluorescence microscope. Kerfoot et al. observed rolling and adhesion of leukocytes in brain postcapillary venules before onset of physical symptoms of MOG-induced EAE in the mouse [58]. Additionally, they indicated that leukocyte–endothelial cell interaction is P-selection/integrin α4 dependent although they did not specify the leukocytes populations. At the same time, Piccio et al. showed that PLP-specific T cells rolled and arrested on the preactivated endothelial cells [59]. They showed importance of selectins/integrins for the interaction. Engelhardt and colleagues employed intravital imaging of encephalitogenic T cells at the BBB [60]. In these studies, activated proteolipid protein-reactive T cell blasts of SJL/N mice were infused intra-arterially, and the migratory behavior of T cells arriving in pial vessels of the spinal cord was analyzed immediately after the T cell injection with a fluorescence video microscope. These newly arriving T cells did not roll along the inner endothelium before getting attached. Instead, they became immediately firmly arrested and penetrated into the CNS parenchyma within hours after T cell transfer. The process of getting cells arrested on the luminal endothelium was dependent on very late activation antigen 4 (VLA-4)/VCAM-1 interactions, i.e., blocking antibodies reduced significantly the number of adhering and transmigrating T cells [61]. In a recent study, Bauer et al. confirmed that integrin-binding forces were essential for this behavior: integrin-β1-deficient murine T cells lacked the capacity to firmly adhere to CNS microvessels [62].

An unexpected locomotion pattern at the BBB: intraluminal T cell crawling

We investigated the migratory behavior of brain antigen (MBP)-specific T cells in vivo during transfer EAE of the Lewis rat. In contrast to preceding studies where T cells were injected into the CNS arteries and examined immediately after transfer of the activated T cell blasts, we transferred activated T cells i.v. and observed their behavior in vivo for several days. T cells arrived at the BBB after i.v. transfer as postactivated migration-competent effector T cells, i.e., after they had proceeded along distinct migratory paths through secondary lymphatic organs during the preclinical phase of EAE. The effector T cells underwent profound functional changes on their way to the CNS [15]. This "migratory" phenotype included downregulation of activation markers (OX-40 antigen, interleukin (IL)-2 receptor, IFNγ, IL-17) and upregulation of chemokine receptors (CCR5, CCR2).

Very few $T_{MBP\text{-}GFP}$ cells had arrived at leptomeningeal vessels by 24 h p.t., i.e., 2 days before the onset of the clinical disease. $T_{MBP\text{-}GFP}$ cells abounded in the vicinity of blood vessels and moved for extended periods of time along these vessels. $T_{MBP\text{-}GFP}$ cells flowing in the blood stream were too fast to be detected by the TPLSM setting. Rolling cells in these recordings resembled a rope of pearls (Fig. 2b) because the images were averaged several times in the same plane and, thus, one and the same cell was recorded several times on its way at the intraluminal endothelium. The numbers of arriving T cells very slowly increased until 48–60 h p.t., and then we observed a sudden accumulation of the T cells. Intriguingly, the vast majority of the early arriving T cells crawled strictly within the outline of vessels. Therefore, one of our goals was to determine whether the $T_{MBP\text{-}GFP}$ cells were located inside or outside the blood vessels. Several lines of evidence showed that these $T_{MBP\text{-}GFP}$ cells indeed crawled along the intraluminal surface of the vessels [28]. Some $T_{MBP\text{-}GFP}$ cells were shown to arrive via the blood stream, and these T cells started to crawl immediately after becoming attached to the inner surface. Conversely, other T cells were observed to be washed away by the blood stream after they had spent some time crawling within the vessels. In addition, some $T_{MBP\text{-}GFP}$ cells looked like spared black

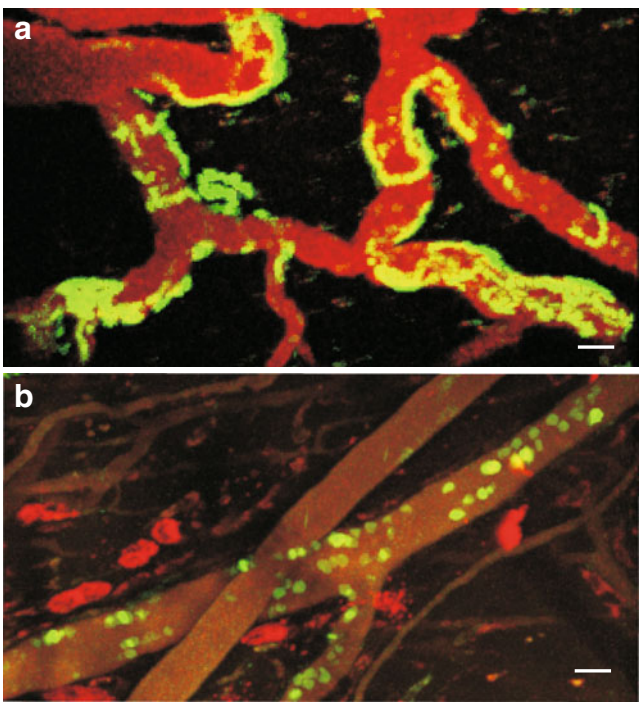

Fig. 2 Intravital recording of $T_{MBP\text{-}GFP}$ cells (*green*) in vessels of the CNS (**a**) and the ear (**b**). Vessels were marked by i.v. injection of Texas Red dextran conjugates (*red*). Thirty-minute movies, consisting of 60 time points, were time-projected. Crawling T cells appear as *continuous lines*, whereas rolling cells appear as *round-shaped dots*. *Scale bar* 30 μm

spots when the detection of the fluorescence of T cells was switched off. Since $T_{MBP\text{-}GFP}$ cells do not take up the dextran label floating within the blood stream, intraluminal $T_{MBP\text{-}GFP}$ cells produce such dark spots, whereas extravasated $T_{MBP\text{-}GFP}$ cells do not. Finally, a 3D reconstruction of the recorded images revealed that indeed many of these early arriving $T_{MBP\text{-}GFP}$ cells were located inside the vessels.

Quantification of crawling vs. rolling cells revealed that more than 80% of the observed $T_{MBP\text{-}GFP}$ cells crawled in the CNS blood vessels. This locomotion behavior was specific to leptomeningeal vessels (Fig. 2a). It was less obvious in the vessels of connective ear tissue, cremasteric muscles, or peripheral nerves (Fig. 2b). Mouse effector T cells and long-lived rat memory/effector T cells were also shown to crawl along the intraluminal surface of the CNS vessels. Furthermore, this intraluminal crawling behavior was not specific to autoantigen-specific T cells. T cells that recognized ovalbumin (OVA; $T_{OVA\text{-}GFP}$ cells) showed a similar pattern of intraluminal crawling. Notably, $T_{OVA\text{-}GFP}$ cells crawled for a shorter time period than their pathogenic counterparts. This was most likely due to the activation state of the endothelium: after cotransfer of pathogenic T_{MBP} cells, the intraluminal crawling time of $T_{OVA\text{-}GFP}$ cells significantly increased and was almost identical to that of $T_{MBP\text{-}GFP}$ cells. The half-life of $T_{MBP\text{-}GFP}$ cell crawling was approximately 15 min [28]. One can speculate with high probability that the $T_{MBP\text{-}GFP}$ cells crawled extensively on the inner surface of CNS vessels in order to spot a suitable place for extravasation.

A closer analysis of the T cell motility at the CNS vessels revealed some more interesting findings [28]. First, intraluminal $T_{MBP\text{-}GFP}$ cells moved preferably in the opposite direction to the blood flow. Approximately 40% of analyzed cells moved against the blood flow. In contrast, only 20% of the analyzed cells moved in the direction of the blood stream. Extravasated cells did not show any preferential direction. Then, even if intraluminal $T_{MBP\text{-}GFP}$ cells moved against the blood flow, they moved as fast as $T_{MBP\text{-}GFP}$ cells that moved with the blood flow. The average motility of $T_{MBP\text{-}GFP}$ cells was 12 μm/min, independent of their direction. The velocity of intraluminal and extravasated cells was similar. However, intraluminally migrating cells moved slightly faster (12.5 vs. 11.3 μm/min).

Intraluminal crawling is not a specialty of T cells. Monocytes [63], NKT cells [64], and neutrophils [65] also engage in intraluminal crawling. The molecular mechanism of this crawling is not yet completely clear; however, LFA-1 and CX3CR-1 molecules were described to mediate crawling of macrophages, whereas Mac-1 was found to be crucial in neutrophils. We found that VLA-4, but not LFA-1, played an important role in the intraluminal crawling of effector T cells. When anti-VLA-4 antibody was applied i.v., intraluminally crawling $T_{MBP\text{-}GFP}$ cells detached themselves within minutes, and subsequent infiltration and clinical symptoms were strongly reduced [28].

Extravasation followed intraluminal crawling. According to our observations, intraluminally crawling cells stopped abruptly and then immediately changed their shapes, as if looking for an exit. When the place was found, they started to extravasate, a process that took approximately 10–20 min [28]. The detailed molecular mechanisms underlying diapedesis are still unclear, but integrins and G-coupled proteins were shown to contribute to T cell extravasation [62, 66]. Engelhardt et al. [67] suggested that there are two different ways of extravasation, namely either paracellular migration, during which T cells pass through the tight junctions between endothelial cells, or transcellular migration, during which T cells pass though endothelial cells as in endocytosis and exocytosis. It is yet to be clarified which of these two ways characterize rat autoreactive T cells.

Encountering the gatekeepers in perivascular/meningeal locations: a crucial checkpoint for parenchymal invasion

It was known that once the effector T cells had overcome the vascular barrier of the CNS vessels, they would become reactivated, i.e., they expressed membranous activation markers (OX-40 antigen and IL-2 receptor) and released proinflammatory cytokines [15, 68]. The CNS, as well as the eyes and the testes, are commonly considered immune-privileged environments due to the lack of professional APCs and lymphatic vessels [69]. Over the last decades, however, this view has been challenged. For example, it turned out that, upon stimulation with proinflammatory cytokines, soluble mediators, such as chemokines and cytokines, as well as MHC determinants can be induced on many, if not all, brain cells [70]. However, it still remains open which cell type accounts for the reactivation of effector T cells freshly arriving at the naive BBB. Perivascular/meningeal macrophages are known to constitutively express MHC class II molecules and to present endogenous autoantigens [71]. Indeed, our intravital imaging studies hinted to a crucial role of this phagocyte population in the activation process of T cells.

Our intravital recordings also revealed that $T_{MBP\text{-}GFP}$ cells after diapedesis stayed in the vicinity of the blood vessels and continued to crawl on the abluminal surface. A quantitative analysis showed that freshly extravasating T cells spend 80% of their time in the perivascular locations [28]. Because $T_{MBP\text{-}GFP}$ cells were activated immediately after leaving the blood circulation, we hypothesized that $T_{MBP\text{-}GFP}$ cells were activated in the perivascular locations

when they come in contact with resident APCs. Previous studies demonstrated that in the perivascular area of leptomeningeal vessels there are indeed potential APCs. These APCs were found to be radiosensitive [71]. To make these cells visible for TPLSM, we therefore prepared bone marrow chimeras, in which bone marrow cells derived from GFP transgenic rats [21] were grafted into lethally irradiated wild-type recipient rats. The animals were kept at least 10 weeks to allow sufficient replacement of the perivascular cells and were then used in the experiments [72]. Alternatively, we injected fluorescent-conjugated dextran intrathecally into the cisterna magna to light up the phagocytic cells in the CNS perivascular areas and the meninges. Both methods stained a similar population of cells. Although the number of labeled phagocytic cells exceeded those of bone-marrow-derived cells, we confirmed that the majority (>90%) of bone-marrow-derived cells were labeled with intrathecally injected dye. $T_{MBP\text{-}RFP}$ cells were used in the intravital imaging of GFP bone marrow chimeras. Substantial parts of $T_{MBP\text{-}GFP/RFP}$ cells showed both long stable (>10 min) and multiple short (<10 min) contacts to labeled perivascular macrophages [28]. T cells and dendritic cells in lymph nodes showed similar long- and short-term interactions during intravital imaging, although in a chronologically sequential order [27]. The contact durations in the perivascular/meningeal areas varied at different stages of the autoimmune process: a short series of contacts occurred in the early EAE states, whereas long-lasting contacts became more prominent at a later stage. The meaning of these different contact durations is currently being investigated. Interestingly, not all of the infiltrated $T_{MBP\text{-}GFP}$ cells made stable contacts to antigen-presenting cells (maximally 30–40%) [28]. When soluble MBP was applied intravenously, our intravital recording showed a dramatic increase of arrested $T_{MBP\text{-}GFP}$ cells (>70%) [73]. This indicates that, even during full-blown disease, the antigen-presenting cells in the CNS are not saturated by endogenous autoantigens.

Following their perivascular accumulation and making contacts with potential APCs, $T_{MBP\text{-}GFP}$ cells detached themselves from the blood vessels and migrated freely into the CNS meninges. Furthermore, some T cells started to distribute themselves within the CNS parenchyma [28]. Although T cell–APC contacts and T cell penetration into the CNS occurred, no direct evidence was found for a causal relation between these events. Since $T_{MBP\text{-}GFP}$ cells recognize endogenous MBP-presenting APCs, it was difficult to observe the entire process from antigen recognition to penetration into the CNS. To prove that antigen presentation at the perivascular/meningeal level was sufficient to activate the T cells and their migration, we analyzed the conditions under which brain antigen-ignorant $T_{OVA\text{-}GFP}$ cells would invade the CNS parenchyma.

$T_{OVA\text{-}GFP}$ cells arrive at the vessels of the CNS meninges, but they never spontaneously penetrate in detectable numbers into the parenchyma [15] although a few cells were observed at the perivascular area [28]. To prove the importance of antigen presentation at this location, perivascular/meningeal APCs, which were fed before with ovalbumin, were applied intrathecally into animals 3 days after the transfer of $T_{OVA\text{-}GFP}$ cells. The APCs had been prepared from CNS meninges of naïve Lewis rats by flow cytometric sorting of fluorochrome-conjugated dextran-labeled cells. These APCs carry markers of macrophages, i.e., they expressed CD11b but not CD11c (dendritic cell marker), T cell receptor, OX-33 (B cell marker), or RECA1 (endothelial cell marker). Most importantly, more than half of these labeled cells expressed MHC class II and could stimulate T cells in an antigen-specific manner in vitro. Intriguingly, the OVA-pulsed APC recruited high numbers of $T_{OVA\text{-}GFP}$ cells into CNS parenchyma. Additionally, intravital recording revealed that $T_{OVA\text{-}GFP}$ cells after transfer of the OVA-pulsed APC got arrested to the cells and developed signs of efficient reactivation. Furthermore, OVA-pulsed APC-treated animals revealed mild clinical symptoms, i.e., they suffered significant weight loss. These data provide strong evidence that APCs located in perivascular/meningeal locations are able to activate antigen-specific T cells and to recruit them into the CNS parenchyma, which is followed by the onset of clinical symptoms (Fig. 3) [28].

The above studies indicate that T cells infiltrate the CNS parenchyma via meningeal vessels. In contrast, Reboldi et al. provided evidence for an alternative path via vessels of the choroid plexus [74]. Using CCR6 knockout mice, which are resistant to EAE, they made two findings. First, they found that CCL20, a CCR6 ligand, was expressed in epithelial cells of the choroid plexus in mice and humans. Furthermore, lymphocytes were found to accumulate at the choroid plexus in CCR6-deficient mice. Taken together, they suggested that T cells initially start to penetrate into the CNS via the choroid plexus in a CCL20-CCR6-dependent manner. Additionally, they reconstituted EAE susceptibility by transferring wild-type T cells; afterwards, even CCR6-deficient T cells penetrated into the CNS. This result suggested that CCR6 plays an important role in the initiation of the disease, but once the blood brain barrier is disrupted, other T cells pass into the CNS independently of CCR6.

$T_{MBP\text{-}GFP}$ cell motility deep within the CNS parenchyma

Due to limited penetration depth, TPLSM is not suitable for obtaining images deep inside the CNS parenchyma. Therefore, CNS explants were imaged [75]. CNS acute

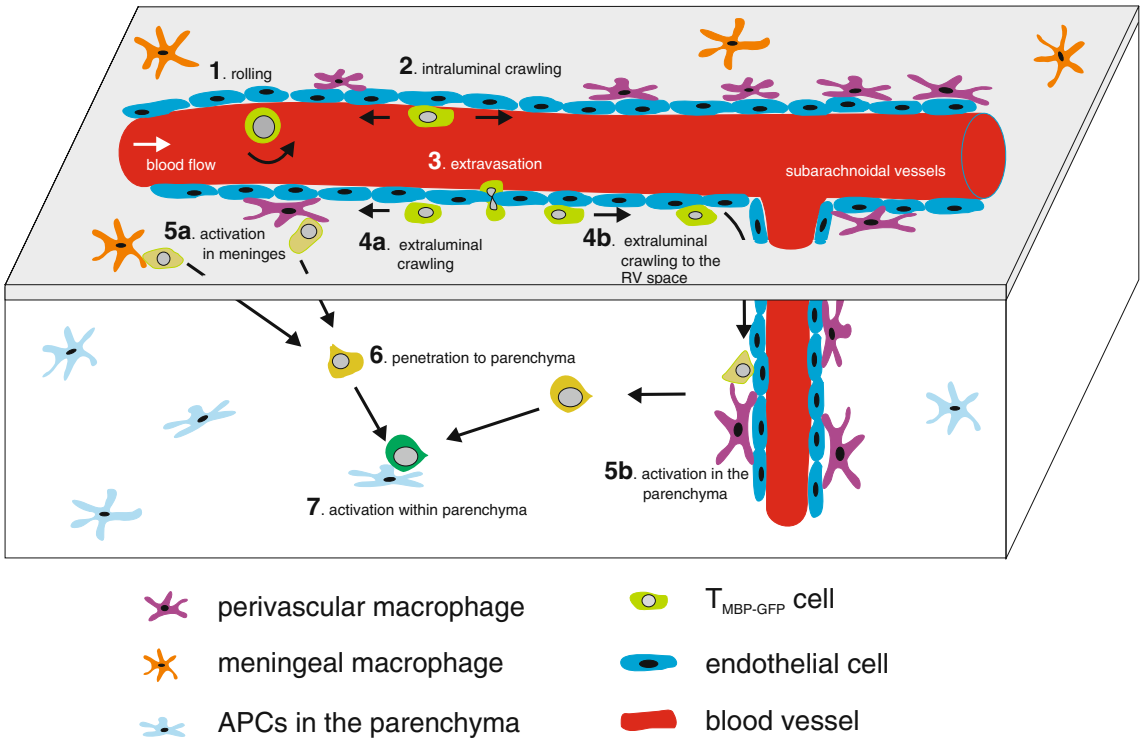

Fig. 3 Schema of the invasion steps of $T_{MBP\text{-}GFP}$ cells into the CNS parenchyma. $T_{MBP\text{-}GFP}$ cells arrive at CNS leptomeningeal vessels and roll on endothelial cells (*1*). This is followed by intraluminal crawling directed both upstream and downstream of blood flow (*2*). After the extravasation (*3*), $T_{MBP\text{-}GFP}$ cells continue to crawl to the abluminal surface of vessels (*4a*). A part of T cells dive to the Robin Virchow space (*RV*; *4b*). T cells meet local antigen-presenting cells at the perivascular space of leptomeningeal vessels (*5a*) or parenchyma (*5b*) and are activated. Activated T cells are allowed to penetrate within the CNS parenchyma (*6*). Finally, T cells can be further activated by antigen-presenting cells in the CNS parenchyma (*7*)

slices with a thickness of 300 μm were prepared from the acute phase of EAE rats. Explants were placed in custom-made chambers in which temperature-controlled oxygen-enriched buffer was constantly perfused. This setting allowed us to visualize T cell motility within the CNS parenchyma for a number of hours.

$T_{MBP\text{-}GFP}$ cells moved very fast in the CNS parenchyma, reaching velocities of maximally 25 μm/min, i.e., they traveled almost as fast as T cells in the lymph nodes [37]. This finding was surprising if one considers the compactness and the highly structured composition of the CNS parenchyma, which lack preformed "roads" for immune cells. The T cells moved in all directions, apparently ignoring chemokine gradients, although chemokines might exert an influence in microenvironments. The cells do not move spontaneously but rather moved in a "stop-and-go" mode, which suggested a possible interaction with local structures. Two types of T cell motility were found: motile and stationary. Two thirds of the cells showed the motile phenotype, moving more than 10 μm in 10 min. Mean displacement analysis revealed that they exhibited a "random walk." The remaining cells showed the stationary phenotype, their locomotion being highly confined. These effector T cells seemed to be anchored at a fixed point and moved the rest of their cell body around this fixation. Some motile cells changed to stationary or vice versa.

We speculated that the stationary T cells were in the process of antigen recognition, whereas motile cells were on the search for APCs presenting their antigen. Several arguments supported this hypothesis. First, $T_{OVA\text{-}GFP}$ cells recruited into the CNS parenchyma by cotransfer of $T_{MBP\text{-}GFP}$ cells showed hardly any stationary phenotype, most likely since ovalbumin is not presented within the CNS tissue. Second, $T_{OVA\text{-}GFP}$ cells became arrested in the CNS parenchyma, when ovalbumin was provided to APCs of the spinal cord. Inversely, the numbers of stationary $T_{MBP\text{-}GFP}$ cells were reduced when neutralizing anti-MHC class II monoclonal antibody was applied in the CNS. Third, stationary cells were observed to make immunological synapses [53, 76, 77] and move around their anchor point. These results strongly suggest that the cells were stationary during the process of antigen recognition.

Antigen recognition preceded T cell activation, which was followed by the production of inflammatory chemokines, including TNFα, MIP1α, and MCP1. Only activated T cells produce these chemokines. For example, low-pathogenic S100β or MOG-specific T cells, which are not/insufficiently activated in the CNS, did not produce these inflammatory

cytokines [68] although both types of T cells could penetrate into the CNS. The upregulated inflammatory cytokines recruit macrophages, which contributed to the development of EAE clinical symptoms.

Outlook for the future

Recent developments in technical instruments and fluorescent reporter dyes and technologies now provide researchers with previously unimagined possibilities. Intravital imaging by two-photon microscopy started with the observation of a single-cell population, i.e., lymphocytes, in organ explants. Soon thereafter, tracking of interactions between several cell types, e.g., T cells and dendritic cells, became feasible. Imaging proceeded to intravital imaging at greater depth and for longer periods of observation. Since multicolor imaging in the living animal has become standard, many advances have been made in imaging, for example high-resolution imaging for evaluation of cell function, e.g., calcium signaling, and molecular interaction in the cells. Obviously, each new advance can provide new insights into cells and mechanisms of disease. In summary, intravital imaging has led to a better understanding of immune cell behavior and function in vivo. Studies employing novel or established therapeutic agents, such as anti-VLA-4 antibodies, might additionally add to the development of safer and more targeted therapeutic approaches for autoimmune-mediated diseases.

Acknowledgements This work was supported by the Deutsche Forschungsgemeinschaft SFB571-C6, SFB-TR43-B2, the Multiple Sclerosis competence network "Understand MS," and the Hertie Foundation. We thank Dr. Hartmut Wekerle for his helpful comments. We acknowledge the secretarial assistance of Mrs. Cathy Ludwig.

References

1. Hickey WF, Osborn JP, Kirby WM (1985) Expression of Ia molecules by astrocytes during acute experimental allergic encephalomyelitis in the Lewis rat. Cell Immunol 91:528–535
2. Traugott U, Scheinberg LC, Raine CS (1985) On the presence of Ia-positive endothelial cells and astrocytes in multiple sclerosis lesions and its relevance to antigen presentation. J Neuroimmunol 8:1–14
3. Gold R, Linington C, Lassmann H (2006) Understanding pathogenesis and therapy of multiple sclerosis via animal models: 70 years of merits and culprits in experimental autoimmune encephalomyelitis research. Brain 129:1953–1971
4. Freund J, Stern ER, Pisani TM (1947) Isoallergic encephalomyelitis and radiculitis in Guinea pigs after one injection of brain and mycobacteria in water-in-oil emulsion. J Immunol 57:179–195
5. Ben-Nun A, Wekerle H, Cohen IR (1981) The rapid isolation of clonable antigen-specific T lymphocyte lines capable of mediating autoimmune encephalomyelitis. Eur J Immunol 11:195–199
6. Kies MW, Murphy JB, Alvord EC (1960) Fractionation of guinea pig basic proteins (MBP) with encephalitogenic properties. Fed Proc 22:216
7. Poduslo JF, McFarlin DE (1978) Immunogenicity of a membrane surface glycoprotein associated with central nervous system myelin. Brain Res 159:234–238
8. Williams RM, Lees MB, Cambi F, Macklin WB (1982) Chronic experimental allergic encephalomyelitis induced in rabbits with bovine white matter proteolipid apoprotein. J Neuropathol Exp Neurol 41:508–521
9. Paterson PY (1960) Transfer of allergic encephalomyelitis in rats by means of lymph node cells. J Exp Med 111:119–135
10. Gonatas NK, Howard JC (1974) Inhibition of experimental allergic encephalomyelitis in rats severely depleted of T cells. Science 186:839–841
11. Ben-Nun A, Wekerle H, Cohen IR (1981) Vaccination against autoimmune encephalomyelitis using attenuated cells of a T lymphocyte line reactive against myelin basic protein. Nature 292:60–61
12. Hickey WF, Hsu BL, Kimura H (1991) T lymphocyte entry into the central nervous system. J Neurosci Res 28:254–260
13. Hickey WF (1999) Leukocyte traffic in the central nervous system: the participants and their roles. Semin Immunol 11:125–137
14. Flügel A, Willem M, Berkowicz T, Wekerle H (1999) Gene transfer into $CD4^+$ T lymphocytes: green fluorescent protein engineered, encephalitogenic T cells used to illuminate immune responses in the brain. Nat Med 5:843–847
15. Flügel A, Berkowicz T, Ritter T, Labeur M, Jenne D, Li Z, Ellwart J, Willem M, Lassmann H, Wekerle H (2001) Migratory activity and functional changes of green fluorescent effector T cells before and during experimental autoimmune encephalomyelitis. Immunity 14:547–560
16. Lyons AB, Parish CR (1994) Determination of lymphocyte division by flow cytometry. J Immunol Meth 171:131–137
17. Miller MJ, Wei SH, Cahalan MD, Parker I (2003) Autonomous T cell trafficking examined in vivo with intravital two-photon microscopy. Proc Natl Acad Sci U S A 100:2604–2609
18. Marshall J, Molloy R, Moss GWJ, Howe JR, Hughes TE (1995) The jellyfish green fluorescent protein: a new tool for studying ion channel expression and function. Neuron 14:211–215
19. Heim R, Cubitt AB, Tsien RY (1995) Improved green fluorescence. Nature 373:663–664
20. Kawakami N, Sakane N, Nishizawa F, Iwao M, Fukuda S, Tsujikawa K, Kohama Y, Ikawa M, Okabe M, Yamamoto H (1999) Green fluorescent protein-transgenic mice: immune functions and their application to studies of lymphocyte development. Immunol Lett 70:165–171
21. Lois C, Hong IJ, Pease S, Brown EJ, Baltimore D (2002) Germ line transmission and tissue-specific expression of transgenes delivered by lentiviral vectors. Science 295:868–872
22. Miyawaki A, Sawano A, Kogure T (2003) Lighting up cells: labelling proteins with fluorophores. Nat Cell Biol 5:S1–S7
23. Matz MV, Fradkov AF, Labas YA, Savitsky AP, Zaraisky AG, Markelov ML, Lukyanov SA (1999) Fluorescent proteins from nonbioluminescent *Anthozoa* species. Nat Biotech 17:969–973
24. Tomura M, Yoshida N, Tanaka J, Karasawa S, Miwa Y, Miyawaki A, Kanagawa O (2008) Monitoring cellular movement in vivo

with photoconvertible fluorescence protein "Kaede" transgenic mice. Proc Natl Acad Sci U S A 105:10871–10876
25. Shaner NC, Steinbach PA, Tsien RY (2005) A guide to choosing fluorescent proteins. Nat Meth 2:905–909
26. Zipfel WR, Williams RM, Christie R, Nikitin AY, Hyman BT, Webb WW (2003) Live tissue intrinsic emission microscopy using multiphoton-excited native fluorescence and second harmonic generation. Proc Natl Acad Sci U S A 100:7075–7080
27. Mempel TR, Henrickson SE, von Andrian UH (2004) T-cell priming by dendritic cells in lymph nodes occurs in three distinct phases. Nature 427:154–159
28. Bartholomäus I, Kawakami N, Odoardi F, Schläger C, Miljkovic D, Ellwart JW, Klinkert WEF, Flügel-Koch C, Issekutz TB, Wekerle H, Flügel A (2009) Effector T cell interactions with meningeal vascular structures in nascent autoimmune CNS lesions. Nature 462:94–98
29. Shakhar G, Lindquist RL, Skokos D, Dudziak D, Huang JH, Nussenzweig MC, Dustin ML (2005) Stable T cell–dendritic cell interactions precede the development of both tolerance and immunity in vivo. Nat Immunol 6:707–714
30. Nimmerjahn A, Kirchoff F, Kerr JND, Helmchen F (2004) Sulforhodamine 101 as a specific marker of astroglia in the neocortex in vivo. Nat Med 1:31–37
31. Denk W, Svoboda K (1997) Photon upmanship: why multiphoton imaging is more than a gimmick. Neuron 18:351–357
32. Masters BR, So PT (2004) Antecedents of two-photon excitation laser scanning microscopy. Microsc Res Tech 63:3–11
33. Denk W, Strickler JH, Webb WW (1990) 2-photon laser scanning fluorescence microscopy. Science 248:73–76
34. Niesner R, Andresen V, Neumann J, Spiecker H, Gunzer M (2007) The power of single and multibeam two-photon microscopy for high-resolution and high-speed deep tissue and intravital imaging. Biophys J 93:2519–2529
35. Helmchen F, Fee MS, Tank DW, Denk W (2001) A miniature head-mounted two-photon microscope: high resolution brain imaging in freely moving animals. Neuron 31:903–912
36. Levene MJ, Dombeck DA, Kasischke KA, Molloy RP, Webb WW (2004) In vivo multiphoton microscopy of deep brain tissue. J Neurophysiol 91:1908–1912
37. Miller MJ, Wei SH, Parker I, Cahalan MD (2002) Two-photon imaging of lymphocyte motility and antigen response in intact lymph node. Science 296:1869–1873
38. Bousso P, Bhakta NR, Lewis RS, Robey E (2002) Dynamics of thymocyte–stromal cell interactions visualized by two-photon microscopy. Science 296:1876–1880
39. Bajénoff M, Egen JG, Koo LY, Laugier JP, Brau F, Glaichenhaus N, Germain RN (2006) Stromal cell networks regulate lymphocyte entry, migration, and territoriality in lymph nodes. Immunity 25:989–1001
40. Miller MJ, Safrina O, Parker I, Cahalan MD (2004) Imaging the single cell dynamics of $CD4^+$ T cell activation by dendritic cells in lymph nodes. J Exp Med 200:847–856
41. Worbs T, Mempel TR, Bölter J, von Andrian UH, Förster R (2007) CCR7 ligands stimulate the intranodal motility of T lymphocytes in vivo. J Exp Med 204:489–495
42. Hugues S, Fetler L, Bonifaz L, Helft J, Amblard F, Amigorena S (2004) Distinct T cell dynamics in lymph nodes during the induction of tolerance and immunity. Nat Immunol 5:1235–1242
43. Bousso P, Robey E (2003) Dynamics of $CD8^+$ T cell priming by dendritic cells in intact lymph nodes. Nat Immunol 4:579–585
44. Miller MJ, Hejazi AS, Wei SH, Cahalan MD, Parker I (2004) T cell repertoire scanning is promoted by dynamic dendritic cell behavior and random T cell motility in the lymph node. Proc Natl Acad Sci U S A 101:998–1003
45. Boissonnas A, Fetler L, Zeelenberg IS, Hugues S, Amigorena S (2007) In vivo imaging of cytotoxic T cell infiltration and elimination of a solid tumor. J Exp Med 204:345–356
46. Breart B, Lemaître F, Celli S, Bousso P (2008) Two-photon imaging of intratumoral $CD8^+$ T cell cytotoxic activity during adoptive T cell therapy in mice. J Clin Invest 118:1390–1397
47. Kim JV, Kang SS, Dustin ML, McGavern DB (2009) Myelomonocytic cell recruitment causes fatal CNS vascular injury during acute viral meningitis. Nature 457:191–195
48. Tadokoro CE, Shakhar G, Shen SQ, Ding Y, Lino AC, Maraver A, Lafaille JJ, Dustin ML (2006) Regulatory T cells inhibit stable contacts between $CD4^+$ T cells and dendritic cells in vivo. J Exp Med 203:505–511
49. Qi H, Egen JG, Huang AYC, Germain RN (2006) Extrafollicular activation of lymph node B cells by antigen-bearing dendritic cells. Science 312:1672–1676
50. Qi H, Cannons JL, Klauschen F, Schwartzberg PL, Germain RN (2008) SAP-controlled T–B cell interactions underlie germinal centre formation. Nature 455:764–769
51. Bhakta NR, Oh DY, Lewis RS (2005) Calcium oscillations regulate thymocyte motility during positive selection in the three-dimensional thymic environment. Nat Immunol 6:143–151
52. Wei SH, Safrina O, Yu Y, Garrod KR, Cahalan MD, Parker I (2007) Ca^{2+} signals in $CD4^+$ T cells during early contacts with antigen-bearing dendritic cells in lymph node. J Immunol 179:1586–1594
53. Grakoui A, Bromley SK, Sumen C, Davis MM, Shaw AS, Allen PM, Dustin ML (1999) The immunological synapse: a molecular machine controlling T cell activation. Science 285:221–227
54. Hailman E, Burack WR, Shaw AS, Dustin ML, Allen PM (2002) Immature $CD4^+CD8^+$ thymocytes form a multifocal immunological synapse with sustained tyrosine phosphorylation. Immunity 16:839–848
55. Thauland TJ, Koguchi Y, Wetzel SA, Dustin ML, Parker DC (2008) Th1 and Th2 cells form morphologically distinct immunological synapses. J Immunol 181:393–399
56. Lee K-H, Dinner AR, Tu C, Campi G, Raychaudhuri S, Tarma R, Sims TN, Burack WR, Wu H, Wang J, Kanagawa O, Markiewicz M, Allen PM, Dustin ML, Chakraborty AK, Shaw AS (2003) The immunological synapse balances T cell receptor signaling and degradation. Science 302:1218–1222
57. Kim JV, Jiang N, Tadokoro CE, Liu LP, Ransohoff RM, Lafaille JJ, Dustin ML (2010) Two-photon laser scanning microscopy imaging of intact spinal cord and cerebral cortex reveals requirement for CXCR6 and neuroinflammation in immune cell infiltration of cortical injury sites. J Immunol Meth 352:89–100
58. Kerfoot SM, Kubes P (2002) Overlapping roles of P-selectin and a_4 integrin to recruit leukocytes to the central nervous system in experimental autoimmune encephalomyelitis. J Immunol 169:1000–1006
59. Piccio L, Rossi B, Scarpini E, Laudanna C, Giagulli C, Issekutz AC, Vestweber D, Butcher EC, Constantin G (2002) Molecular mechanisms involved in lymphocyte recruitment in inflamed brain microvessels: critical roles for P-selectin glycoprotein ligand-1 and heterotrimeric G(i)-linked receptors. J Immunol 168:1940–1949
60. Engelhardt B, Ransohoff RM (2005) The ins and outs of T-lymphocyte trafficking to the CNS: anatomical sites and molecular mechanisms. Trends Immunol 26:485–495
61. Vajkoczy P, Laschinger M, Engelhardt B (2001) a4-integrin-VCAM binding mediates G protein independent capture of encephalitogenic T cell blasts to CNS white matter microvessels. J Clin Invest 108:557–565
62. Bauer M, Brakebusch C, Coisne C, Sixt M, Wekerle H, Engelhardt B, Fässler R (2009) b1 integrins differentially control extravasation of inflammatory cell subsets into the CNS during autoimmunity. Proc Natl Acad Sci U S A 106:1920–1925
63. Auffray C, Fogg D, Garfa M, Elain G, Join-Lambert O, Kayal S, Sarnacki S, Cumano A, Lauvau G, Geissmann F (2007)

Monitoring of blood vessels and tissues by a population of monocytes with patrolling behavior. Science 317:666–670
64. Geissmann F, Cameron TO, Sidobre S, Manlongat N, Kronenberg M, Briskin MJ, Dustin ML, Littman DR (2005) Intravascular immune surveillance by $CXCR6^{+}$ NKT cells patrolling liver sinusoids. PLoS Biol 3:e113
65. Phillipson M, Heit B, Colarusso P, Liu LX, Ballantyne CM, Kubes P (2006) Intraluminal crawling of neutrophils to emigration sites: a molecularly distinct process from adhesion in the recruitment cascade. J Exp Med 203:2569–2575
66. Engelhardt B (2006) Molecular mechanisms involved in T cell migration across the blood–brain barrier. J Neural Transm 113:477–485
67. Engelhardt B, Wolburg H (2004) Mini-review: transendothelial migration of leukocytes: through the front door or around the side of the house? Eur J Immunol 34:2955–2963
68. Kawakami N, Lassmann S, Li Z, Odoardi F, Ritter T, Ziemssen T, Klinkert WEF, Ellwart J, Bradl M, Krivacic K, Lassmann H, Ransohoff RM, Volk H-D, Wekerle H, Linington C, Flügel A (2004) The activation status of neuroantigen-specific T cells in the target organ determines the clinical outcome of autoimmune encephalomyelitis. J Exp Med 199:185–197
69. Barker CF, Billingham RE (1977) Immunologically privileged sites. Adv Immunol 25:1–54
70. Wong GHW, Bartlett PF, Clark-Lewis I, Battye F, Schrader JW (1984) Inducible expression of H-2 and Ia antigens on brain cells. Nature 310:688–691
71. Hickey WF, Kimura H (1988) Perivascular microglial cells of the CNS are bone-marrow derived and present antigen in vivo. Science 239:290–293
72. Bechmann I, Priller J, Kovac A, Bontert M, Wehner T, Klett FF, Bohsung J, Stuschke M, Dirnagl U, Nitsch R (2001) Immune surveillance of mouse brain perivascular spaces by blood-borne macrophages. Eur J Neurosci 14:1651–1658
73. Odoardi F, Kawakami N, Klinkert WEF, Wekerle H, Flügel A (2007) Blood-borne soluble protein antigen intensifies T cell activation in autoimmune CNS lesions and exacerbates clinical disease. Proc Natl Acad Sci U S A 104:18625–18630
74. Reboldi A, Coisne C, Baumjohann D, Benvenuto F, Bottinelli D, Lira SA, Uccelli A, Lanzavecchia A, Engelhardt B, Sallusto F (2009) C–C chemokine receptor 6—regulated entry of TH-17 cells into the CNS through the choroid plexus is required for the initiation of EAE. Nat Immunol 10:514–523
75. Kawakami N, Nägerl UV, Odoardi F, Bonhoeffer T, Wekerle H, Flügel A (2005) Live imaging of effector cell trafficking and autoantigen recognition within the unfolding autoimmune encephalomyelitis lesion. J Exp Med 201:1805–1814
76. Lanzavecchia A, Sallusto F (2000) From synapses to immunological memory: the role of sustained T cell stimulation. Curr Opin Immunol 12:92–98
77. Donnadieu E, Revy P, Trautmann A (2001) Imaging T cell antigen recognition and comparing immunological and neuronal synapses. Immunol 103:417–425